



King Saud University
Arabian Journal of Chemistry

www.ksu.edu.sa
www.sciencedirect.com



ORIGINAL ARTICLE

A facile designed highly moderate craspedia flowerlike sulphated Bi_2O_3 -fly ash catalyst: Green synthetic strategy for (6*H*-pyrido[3,2-*b*]carbazol-4-yl)aniline derivatives in water

Kannan Thirumurthy, Ganesamoorthy Thirunarayanan *

Department of Chemistry, Annamalai University, Annamalaiagar 608002, India

Received 23 January 2015; accepted 18 April 2015

KEYWORDS

Sulfated Bi_2O_3 -fly ash catalyst;
Water;
(6*H*-pyrido[3,2-*b*]carbazol-4-yl)aniline

Abstract The air pollutant fly ash was facile designed as a green catalyst and practical to organic synthesis. We have designed sulfated Bi_2O_3 -fly ash catalyst (12 wt%) and it was characterized by Fourier transform infrared (FT-IR), confocal Raman, Powder X-ray diffraction (XRD), Field emission electron microscopy (FE-SEM), elemental color mapping, energy-dispersive X-ray spectroscopy (EDS), Transmission electron microscopy (TEM) and Brunauer–Emmett–Teller (BET) techniques. The sulfated Bi_2O_3 -fly ash was found an excellent catalytic application for the synthesis of (6*H*-pyrido[3,2-*b*]carbazol-4-yl)aniline derivatives in water has been described. The synthesized (6*H*-pyrido[3,2-*b*]carbazol-4-yl)aniline derivatives were confirmed by spectral techniques Fourier transform infrared (FT-IR), Nuclear magnetic resonance (NMR) and Liquid chromatography–mass spectrometry (LC–MS). The significant catalytic role of Bi–N interaction was readily form adduct, moreover Bi–O bond was favorable for hydrogen abstraction, dehydration and aromatization. Due to the strong potential, the precise reaction time and high yield have been achieved, which is realized from hot filtration test. The sulfated Bi_2O_3 -fly ash catalyst could be reused for five successive run, the resulting in no appreciable change in the catalytic activity. The crystal phase and surface morphology of fifth run catalyst were examined by powder XRD, FE-SEM, EDS and TEM techniques, and the results revealed no changes in catalyst nature. The sulfated Bi_2O_3 -fly ash catalyst has high efficiency, reusability, good catalytic activity, environmentally harmless and notable potential in industrial applications.

© 2015 Production and hosting by Elsevier B.V. on behalf of King Saud University. This is an open access article under the CC BY-NC-ND license (<http://creativecommons.org/licenses/by-nc-nd/4.0/>).

* Corresponding author. Tel.: +91 4144 231215.

E-mail address: drtnarayanan@gmail.com (G. Thirunarayanan).

Peer review under responsibility of King Saud University.



Production and hosting by Elsevier

1. Introduction

Green chemistry is mainly focused on innovative, simple manner to design the sustainable heterogeneous nanocatalyst and it was applied to organic synthesis (Anastas and Lankey, 2002;

<http://dx.doi.org/10.1016/j.arabjc.2015.04.015>

1878-5352 © 2015 Production and hosting by Elsevier B.V. on behalf of King Saud University.

This is an open access article under the CC BY-NC-ND license (<http://creativecommons.org/licenses/by-nc-nd/4.0/>).

Please cite this article in press as: Thirumurthy, K., Thirunarayanan, G. A facile designed highly moderate craspedia flowerlike sulphated Bi_2O_3 -fly ash catalyst: Green synthetic strategy for (6*H*-pyrido[3,2-*b*]carbazol-4-yl)aniline derivatives in water. Arabian Journal of Chemistry (2015), <http://dx.doi.org/10.1016/j.arabjc.2015.04.015>

Anastas and Beach, 2007; Anastas and Eghbali, 2010). Nanocatalysts have been tremendous the renewable sources and reduction of waste. The development of green processes, and pollutant-free catalysts has great importance in the field of nanocatalysis. The innovative catalytic processes will be simple, economically efficient, and ecofriendly, which produces most desirable products. The nanoparticle's, a notice to the criterion of evolution, role is in green chemistry, their high catalytic activity, recoverability and improving the selectivity (Gładysz, 2002). Recent decades, metal and metal oxide nanoparticle catalysts have been established notable importance in organic synthesis. In our case, thermal power plant solid waste residue of fly ash was selected as reaction catalyst. The fly ash renovation is through, eco-friendly and economic, point certain challenge in research society. Class-C fly ash, is a mixture of various metal oxides viz. silica, alumina, ferric oxide, calcium oxide and other metal oxides (Mn_2O_3) along with mullite, quartz and magnetite (Lodeiro et al., 2007). In the past few years, fly ash has been explored for several applications such as adsorption, (Wang and Wu, 2006) material synthesis such as zeolites (Tanaka et al., 2006), geopolymers (Wang et al., 2007), ceramics (Qian et al., 2006), and catalyst supports. The catalytic nature of fly ash used catalyst for organic synthesis such as Knoevenagel condensation (Jain et al., 2012a,b), Claisen–Schmidt condensation (Jain and Rani, 2011) and our research group previously reported Crossed-Aldol condensation (Thirunarayanan et al., 2012).

In recent years, notable application is in organic synthesis by using water as solvent (Lubineau et al., 1994). Certainly water offers many benefits because it is readily available, non-toxic and non-flammable, economical and an environmental point of view. Ensuing this we have focused on environmental concern, the green reagent of bismuth (III) catalyst. The green reagent bismuth is considered to be safe, easy to handle, non-toxic and non-carcinogenic (Sax and Bewis, 1989a,b). Bismuth (III) has numerous applications in cosmetic, medicinal chemistry, diagnostic and surgical procedures, such as antiseptic during surgeries, Peptobismolt for stomach disorders and treatment of diarrhea (Bothwell et al., 2011). The catalytic application of bismuth (III) compounds in organic synthesis has been reported as several review articles and monographs such as Mukaiyama–aldol reaction and Michael reactions (Roux et al., 1993), β -halo ketones and esters (Roux et al., 1994), α -amidoalkylation (Pin et al., 2007) and Friedel–Crafts acylation (Gmouh et al., 2003).

For the past several years, carbazole derivatives have significantly attracted in synthetic community. Carbazole derivatives possess biologically activity and promising pharmacological activities such as brain tumors (Vistica et al., 1994), HIV (Ding et al., 1992), anticancer (Kizek et al., 2012), antitumour activity (Dalton et al., 1967). Carbazole and its derivatives are also widely used as organic materials due to their photo-physical properties (Dijken et al., 2004).

In the present study, the air pollutant fly ash would be recycling as a heterogeneous catalyst and environmental benign solvent as water for organic synthesis. To the best of our knowledge the first report of facile designed sulfated Bi_2O_3 -fly ash catalyst utilized for the synthesis of (6*H*-pyrido[3,2-*b*]carbazol-4-yl)aniline derivatives in water. Sulfated Bi_2O_3 -fly ash catalyst was reused for fifth reaction runs and it could not cause any loss in the catalytic activity, and attained good

yields. We have designed sulfated Bi_2O_3 -fly ash easily separable, environmentally and economically beneficial catalyst.

2. Results and discussion

2.1. Fourier transform infrared (FT-IR)

The Fourier transform infrared (FT-IR) spectra of fly ash (Class C) and sulfated Bi_2O_3 -fly ash (12 wt%) are shown in Fig. 1a and b. Fig. 1a shows that the broad OH peak was appeared at 3476 cm^{-1} denotes the OH stretching vibration. The powder nature of fly ash is associated with the hydrogen-bonded water molecules (Jain et al., 2012a,b). The broad peak appeared at 1166 cm^{-1} is assigned as asymmetric stretching vibration of sulfate (Liu et al., 2011) which depicted in Fig. 1b. The FT-IR spectrum of Bi_2O_3 two peaks appeared at 473 cm^{-1} and 525 cm^{-1} is due to the stretching vibration of Bi–O bonded of $\alpha\text{-Bi}_2\text{O}_3$ which is also in good agreement with earlier reports (Ai et al., 2011). The stretching vibration mode of Bi–O–Bi appears at 668 cm^{-1} is good agreement with earlier reports (Elkholy et al., 1995).

2.2. Confocal Raman

Confocal Raman spectra of fly ash and sulfated Bi_2O_3 -fly ash are shown in Fig. 2a and b. The fly ash has no significant Raman shift observed, it suggests that because of the amorphous nature of fly ash, no shift was obtained as shown in Fig. 2a. Fig. 2b reveals that the sulfated Bi_2O_3 -fly ash catalyst, the sulfate antisymmetric stretching vibration was observed at 1063 cm^{-1} as good agreement with earlier report in the literature (Dong et al., 2007). The new peak was appeared at 1694 cm^{-1} it corresponds to Bi–O bond stretching vibration (He et al., 2014). The results were seen that the facile designed sulfated Bi_2O_3 -fly ash has good crystalline phase.

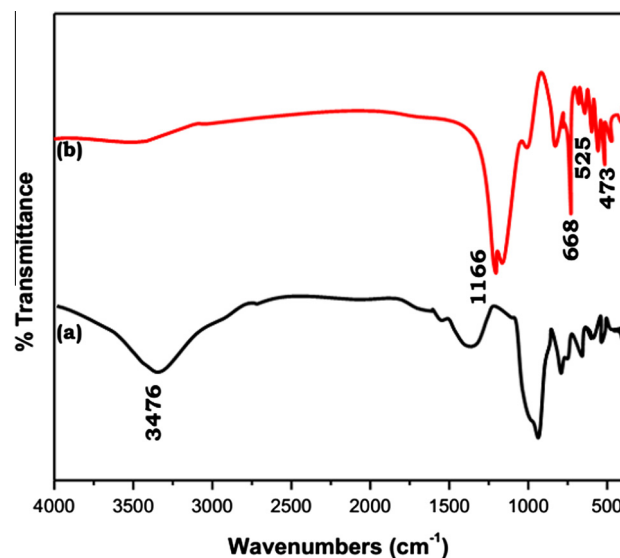


Figure 1 FT-IR spectra of (a) fly ash and (b) sulfated Bi_2O_3 -fly ash.

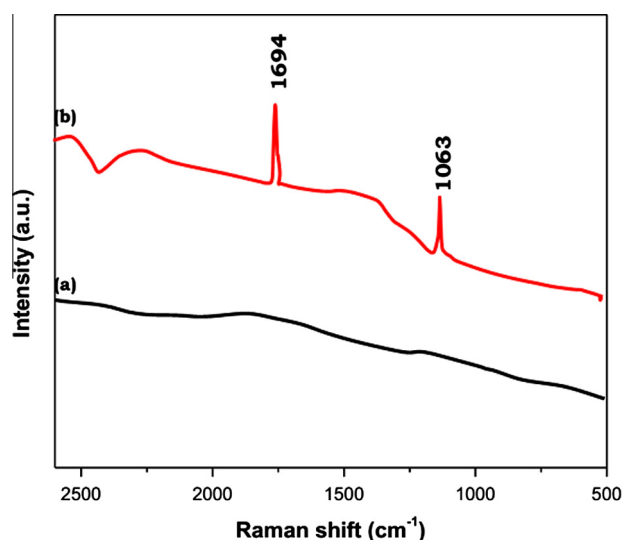


Figure 2 Confocal Raman spectra of (a) fly ash and (b) sulfated Bi_2O_3 -fly ash.

2.3. Powder X-ray diffraction (PXRD)

The crystalline nature of fly ash and sulfated Bi_2O_3 -fly ash (12 wt%) was examined, by powder X-ray diffraction (PXRD) patterns is shown in Fig. 3a and b. The fly ash (Class C) is a mixture of various inorganic oxides viz. silica, alumina, ferric oxide, calcium oxide and other metal oxides (Mn_2O_3 and TiO_2) along with mullite, quartz and calcite which denoted the letters M, Q and C respectively as shown in Fig. 3a and b. Fig. 3b shows the facile designed sulfated Bi_2O_3 -fly ash in the diffraction patterns. The XRD patterns of Bi_2O_3 2θ (degree) values are appeared at 11.86, 31.42, 33.02, 64.21 and 77.82, and the corresponding planes are (110), (222), (122), (444) and (028). The diffraction patterns were good agreement with the literature value for Bi_2O_3 (JCPDS card no-74-1375) (Sillen, 1938).

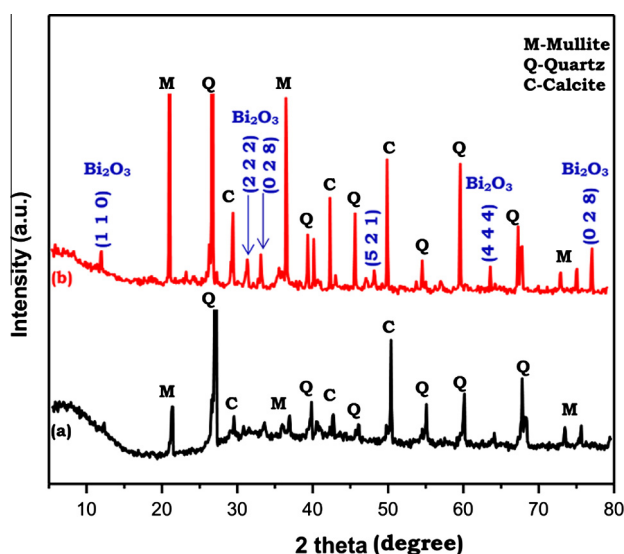


Figure 3 Powder XRD pattern of (a) fly ash and (b) sulfated Bi_2O_3 -fly ash.

2.4. Field emission scanning electron microscopy (FE-SEM)

The morphology of sulfated Bi_2O_3 -fly ash was examined by field emission scanning electron microscopy (FE-SEM) as shown in Fig. 4a–d. As can be seen in Fig. 4a two types of morphology were observed of 1 μm (indicated in green and red spherical in color) respectively. Fig. 4b shows the close-up view on morphology about 2 μm , it is seen that the flowers like morphology were observed channels in a large domain. In this observation, further reviewed individual morphology of dandelion (inserted) was clearly exhibited which is shown in Fig. 4c. Fig. 4d shows that the craspedia flower (inserted) like regular arrangement was observed. The regular arrangement of rod like petals is notable to see that some of relatively rod like particles appeared in Fig. 4d. It is believed that the flower like morphology has strongly bonded with atom which is highly stable in nature, moral active site sulfated Bi_2O_3 -fly ash might have good crystalline nature (Wang et al., 2013).

2.5. FE-SEM elemental color mapping

FE-SEM elemental color mapping reveals that the uniform distribution of the chemical composition of sulfated Bi_2O_3 -fly ash on the surface which is shown in Fig. 5a. The elemental composition of sulfated Bi_2O_3 -fly ash has been examined by energy-dispersive X-ray spectroscopy (EDS) as the results are shown in Fig. 5b. The sulfated Bi_2O_3 -fly ash elements of Ca, O, Fe, Al, Na, Mg, Si, S and Bi are displayed in various colors which are shown in Fig. 5c–k respectively. It is noteworthy that no other elements seen in the modified sulfated Bi_2O_3 -fly ash catalyst reveal the designed catalyst pure in form.

2.6. Transmission electron microscopy (TEM)

The morphology of sulfated Bi_2O_3 -fly ash is examined by Transmission electron microscopy (TEM) analysis as shown in Fig. 6a–d. Fig. 6a shows that the structure length of the microrod is 1.09 μm and width is 0.23 μm . The corresponding fast Fourier transform (FFT) image was inserted which is regular shape of microrod which is indicated by red arrow. In Fig. 6c the single microrod was observed and small particles are present in the surface of microrod that may be the formation of bismuth oxide particles. Fig. 6d shows that the selected area electron diffraction (SAED) pattern of sulfated Bi_2O_3 -fly ash was recorded which seems that the regular, numeral of parallel axis diffraction spots array are preferentially microrod shape (red line). The bright consistent spots confirm the crystalline behavior of sulfated Bi_2O_3 -fly ash good crystalline nature. From the SAED patterns inter planar spacing is 0.712, 0.301, 0.267, 0.145 and 0.122 nm. The corresponding diffraction planes are (110), (222), (122), (444) and (028) of Bi_2O_3 respectively.

2.7. N_2 adsorption–desorption isotherms

The pore structure of sulfated Bi_2O_3 -fly ash catalyst was investigated by N_2 adsorption–desorption isotherms. The corresponding pore size distribution and specific surface area were examined by the Barrett–Joyner–Halenda (BJH) method and Brunauer–Emmett–Teller (BET) method respectively. The N_2 adsorption–desorption isotherms and BJH description pore

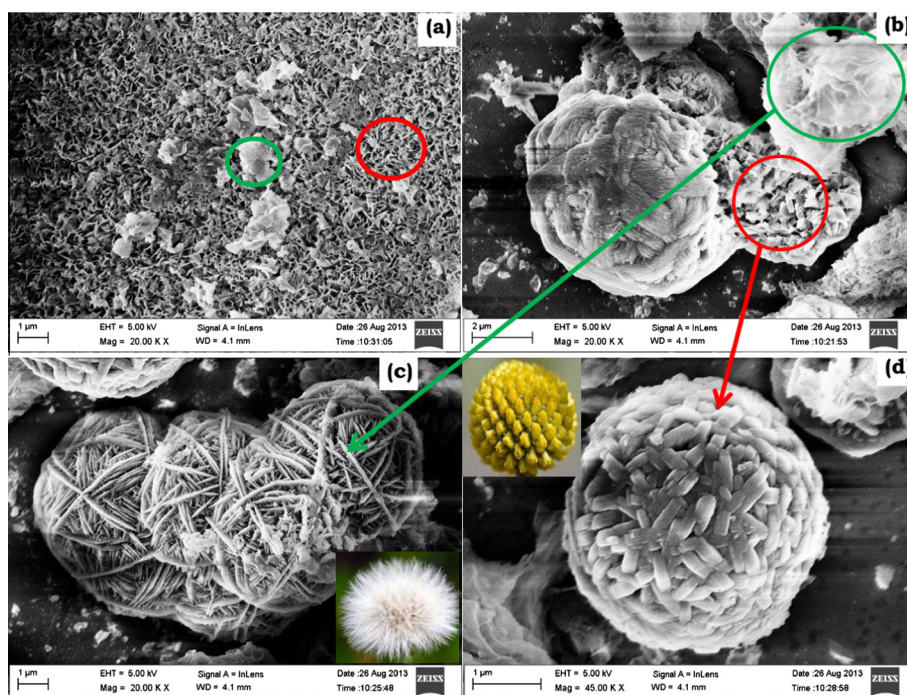


Figure 4 FE-SEM images of sulfated Bi_2O_3 -fly ash scale bars (a) 1 μm , (b) 2 μm , (c) 1 μm (Dandelion flower inserted), and (d) 1 μm (Craspedia flower inserted).

size distribution curve are shown in Fig. 7. This isotherm could be categorized as a typical Type III isotherm according to the classification of IUPAC (Sing et al., 1985). Fig. 7 shows a pore size distribution of sulfated Bi_2O_3 -fly ash which is obtained from the corresponding desorption branch of the N_2 isotherm, by the BJH method. The sulfated Bi_2O_3 -fly ash possesses BET surface area of $5.87 \text{ m}^2/\text{g}$. The absorption of the sulfated Bi_2O_3 -fly ash results shows the nonporous structure and small surface area (Xie et al., 2013). Total pore volume for pores with radius less than 1053.06 \AA at $P/P_0 = 0.990813$ is $2.15 \text{ cm}^3/\text{g}$. The quantitative textural information of the as-designed sulfated Bi_2O_3 -fly ash is BET surface areas, total pore volume 0.023 and pore radius 18.0.

2.8. Optimization of the catalyst

At first we have examined the reaction of for the preparation of **3a** with (*E*)-1-(4-aminophenyl)-3-phenylprop-2-en-1-one (1 mmol), 3-amino-9-ethylcarbazole (1 mmol) and water (20 mL) in the absence of catalyst at 95°C for 12 h. In this reaction condition, no product was obtained Table 1 entry 1. Next, we have examined the reaction in the presence of metal oxide catalyst CuO at 85°C for 8 h. The yield was obtained 18% Table 1 entry 2. We have also examined the reaction in the presence of H_2SO_4 at 85°C for 7 h. The desired product was isolated and the yield is (26%) Table 1 entry 3. From the results, we have preferred further, design of solid phase sulfated fly ash catalyst. The catalytic activity of sulfated fly ash was found for the reaction at 95°C for 12 h. The furnished yield could reach 37% Table 1 entry 5. Our optimization studies have preferred metal oxides loaded fly ash catalyst such as Bi_2O_3 -fly ash and CuO-fly ash. The significant product yield was observed in the Bi_2O_3 -fly ash catalyst (50%) Table 1 entry

6. Considering the favorable reaction condition, concise of Bi_2O_3 -fly ash and sulfated fly ash was shown in Table 1 entry 5 and entry 6. In this observation, the reaction was carried out using different weight percentage of the sulfated Bi_2O_3 -fly ash catalyst (8 and 12 wt%) and was designed. The yield progresses are shown in Table 1 entry 8–9.

The scope of the optimal condition further entries was examined such as both electron withdrawing and electron donating substituent groups, the isolated product is shown in Table 2 entry (3a–3g). The electron withdrawing group of (*E*)-1-(4-aminophenyl)-3-phenylprop-2-en-1-one derivatives was smoothly furnished.

2.9. Hot filtration test

The significance of sulfated Bi_2O_3 -fly ash catalyst was examined by hot filtration test for compound **3f**. A mixture of (*E*)-1-(4-aminophenyl)-3-(4-(methylthio)phenyl)prop-2-en-1-one (1 mmol 269 mg), 3-amino-9-ethylcarbazole (1 mmol 210 mg), water (20 mL) and sulfated Bi_2O_3 -fly ash (100 mg) was refluxed at 85°C for 1 h. The reaction was allowed to proceed for first 15 min and then catalyst was filtered off from the reaction mixture. The isolated product yield (40%) was confirmed by ^1H NMR and LC-MS which is given in Figs. S1a and S4a (see Supporting Information). The reaction was continued for another 60 min and monitored, obviously no changes, in the product yield it was confirmed by LC-MS analysis which is given in Fig. S4. In this observation, we concise in the absence of catalyst, and no reaction is obtained which is shown in Fig. S2 (see Supporting Information). Without removal of the catalyst, the reaction was conducted for 60 min. The reaction was monitored, at different time pause in minutes 30 (85%), 45 (90%), and 60 (99%) and furnished

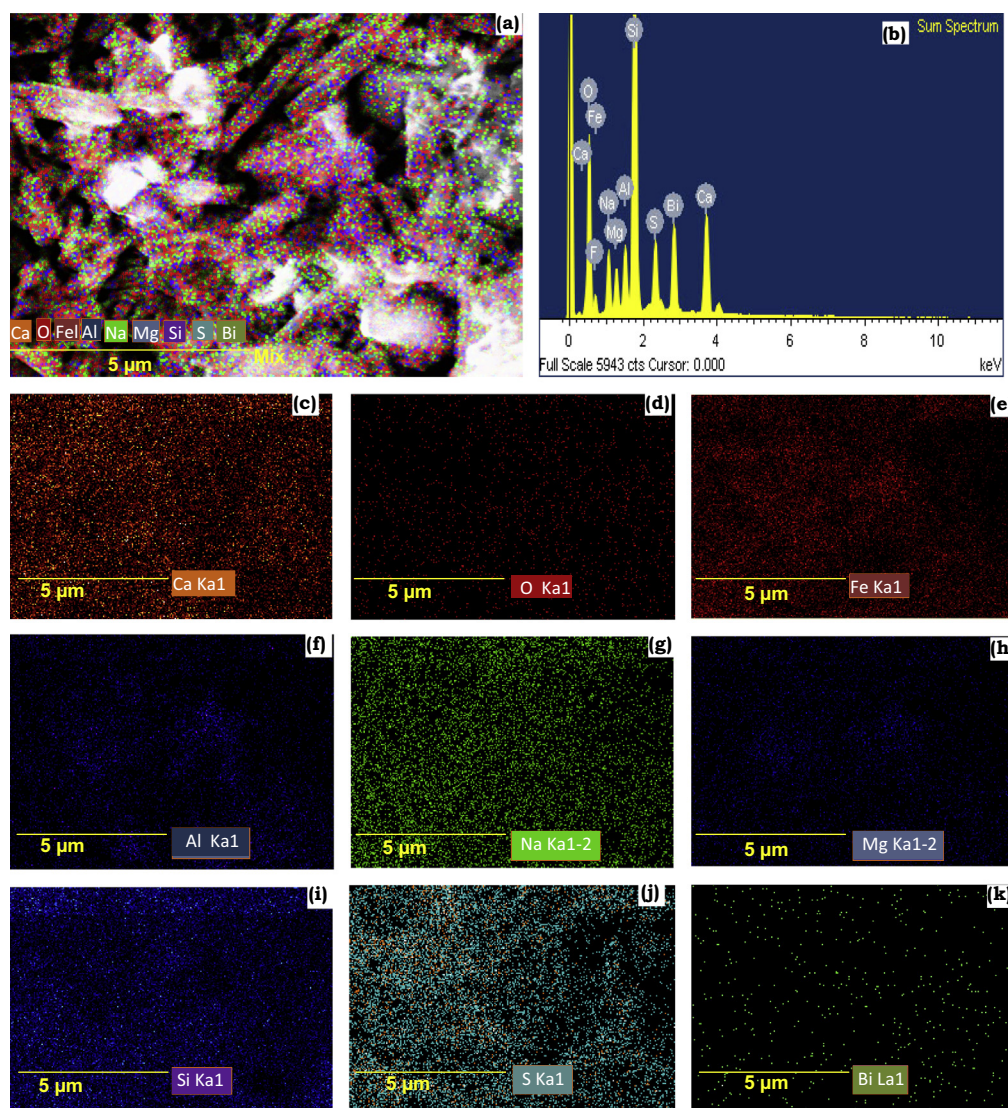


Figure 5 FE-SEM elemental color mapping image of sulfated Bi_2O_3 -fly ash (a) mix color, (b) EDS, (c) Ca, (d) O, (e) Fe, (f) Al, (g) Na, (h) Mg, (i) Si, (j) S, and (k) Bi.

yield is given in Figs. S1 and S4 (see Supporting Information). After 60 min without column chromatographic purification we have attained (99%) yield. The detailed ^1H NMR spectra are given in the Supporting information Fig. S3 (see Supporting Information).

2.10. Reusability of sulfated Bi_2O_3 -fly ash catalyst and its characterization

The catalyst reusability and the efficiency were examined under optimized condition for compound **3f**. The reusability potential of sulfated Bi_2O_3 -fly ash was examined up to five consecutive run. The results seen no appreciable changes in catalytic activity are shown in Fig. 8. The turnover number (TON) and turn over frequency (TOF) are examined and shown in Table 4. The catalyst was separated by filtration method and purified with DCM (30 mL) for unleashed organic substance. Then the catalyst was dried in hot air oven at 130°C for 1 h. The catalytic activity was examined by green matrix method and it was presented in Table 3.

Reused catalyst crystalline and a morphology studies were examined by powder XRD, FE-SEM and TEM. The powder XRD diffraction pattern shows similar than that catalyst which suggests that the there is no appreciable changes in crystallinity and it is shown in Fig. 8a. The surface morphology of fifth reaction run sulfated Bi_2O_3 -fly ash catalyst was examined by FE-SEM. Fig. 8b result reveals that the no appreciable changes in morphology. The elemental composition was confirmed by EDS analysis which is shown in Fig. 8c. The TEM image shows that the rod like morphology observed of $0.5\ \mu\text{m}$, the fast Fourier transform (FFT) images inserted and it is also shown as regular shape of rod (indicated by red arrow).

3. Experimental

3.1. Materials

All chemicals were procured from E-Merck and Sigma-Aldrich India. Fly ash (Class C) was collected from Thermal

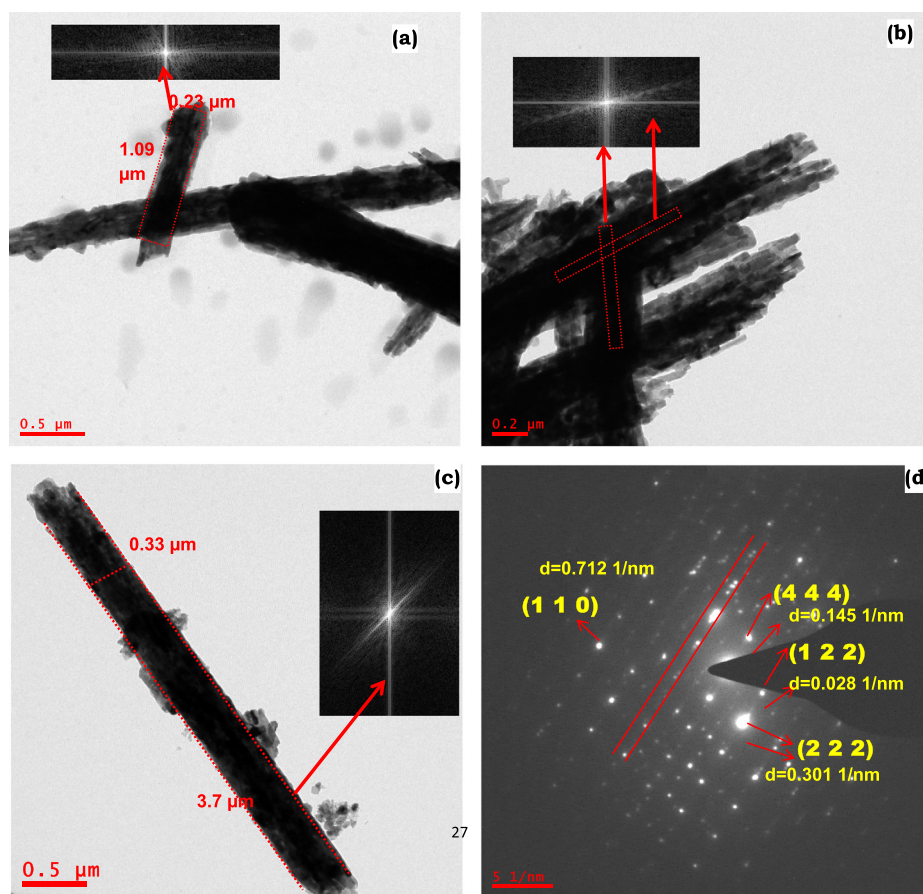


Figure 6 TEM images of sulfated Bi_2O_3 -fly ash (a) 0.5 μm (FFT image inserted), (b) 0.2 μm (FFT image inserted), (c) 0.5 μm rod (FFT image inserted), and (d) SAED pattern 5 1/nm.

Power Plant-II, Neyveli Lignite Corporation (NLC), Neyveli, Tamil Nadu, India.

3.2. Characterization studies

Fourier Transform Infrared spectra (KBr , $4000\text{--}400\text{ cm}^{-1}$) were recorded on a Nicolet-380 Fourier Transform spectrophotometer (FT-IR). Raman spectra were determined in confocal Raman (model witech alpha 300). The Powder X-ray diffraction (XRD) patterns were collected on a D8 Advance Bruker diffractometer operating at 230 V, 50 Hz, 6.5 KVA with $\text{Cu K}\alpha$ source ($\lambda = 1.5418\text{ \AA}$) at room temperature. The surface morphology, size and elemental composition of sulfated Bi_2O_3 -fly ash were characterized by a Field-emission scanning electron microscopy (FE-SEM) recorded on Carl Zeiss (model Ultra 55) and Transmission electron microscopy (TEM) were recorded on (model Tecnai G^2) techniques. The specific surface area of the samples was examined through nitrogen absorption at 77.3 K on the basis of BET equation using a Quantachrome QuadraWin Instruments version 5.02. Melting points of synthesized (6*H*-pyrido[3,2-*b*]carbazol-4-yl)aniline derivatives were determined in open glass capillaries on Mettler FP51 melting point apparatus and are uncorrected. The Nuclear magnetic resonance (NMR) spectra were recorded in Bruker AVIII 5000 instrument operating at 400 MHz (using solvent CDCl_3 tetramethylsilane as internal

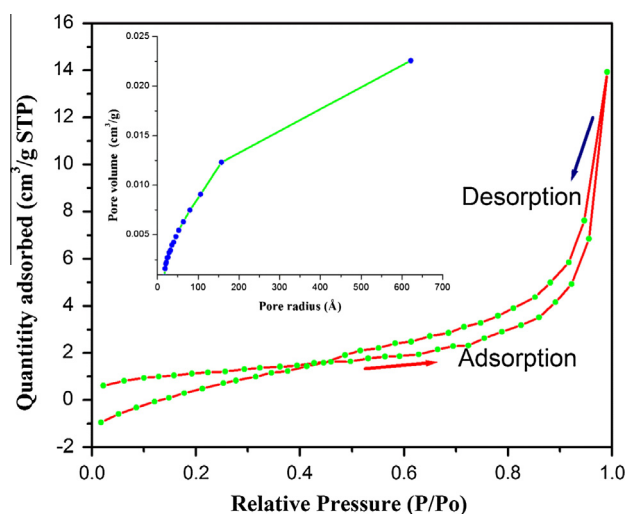


Figure 7 N_2 adsorption-desorption isotherm of the sulfated Bi_2O_3 -fly ash catalyst. Inset of the corresponding pore volume of sulfated Bi_2O_3 -fly ash catalyst.

standard). Liquid chromatography-mass spectrometry (LC-MS) spectra were recorded on a Shimadzu LCMS-2010A model 230VCE.

Table 1 Optimization of catalyst.

Entry	Catalyst	Temperature (°C)	Time (h)	Yield (%)
1	No catalyst	95	12	N.R
2	CuO	85	8	18
3	H ₂ SO ₄	85	7	26
4	Fly ash	95	12	20
5	Sulfated-fly ash	95	12	37
6	Bi ₂ O ₃ -fly ash	85	6	50
7	CuO-fly ash	85	6	30
8	Sulphated Bi ₂ O ₃ -fly ash 8 wt%	85	4	75
9	Sulphated Bi ₂ O ₃ -fly ash 12 wt%	85	4	82

Reaction condition: (*E*)-1-(4-aminophenyl)-3-phenylprop-2-en-1-one (1 mmol), 3-amino-9-ethylcarbazole (1 mmol), in water (20 mL) under reflux.

3.3. Facile design of sulfated Bi₂O₃-fly ash catalyst

The sulfated Bi₂O₃-fly ash catalyst was prepared by hydrothermal method. Fly ash (1000 mg) was taken in clean conical flask and added to 20 mL of ethanol and water, followed by magnetic stirring (600 rpm) at room temperature for 15 min. After 15 min 1.2 mL of 0.05 M sulfuric acid was added to fly ash with vigorous stirring at room temperature for 2 h. Then sulfated fly ash (500 mg) was taken a clean conical flask and mixed with 10 mL of ethanol, stirred for 15 min. Ensuing 112 mg of Bi(NO₃)₃·5H₂O was dissolved in 20 mL of 0.005 M nitric acid to avoiding hydrolyzation of Bi³⁺ ions. The pH level 11 was added adjusted by using 180 mg of urea with constant stirring at 90 °C for 2 h. The resulting yellow color solid was obtained, and it is transferred into a

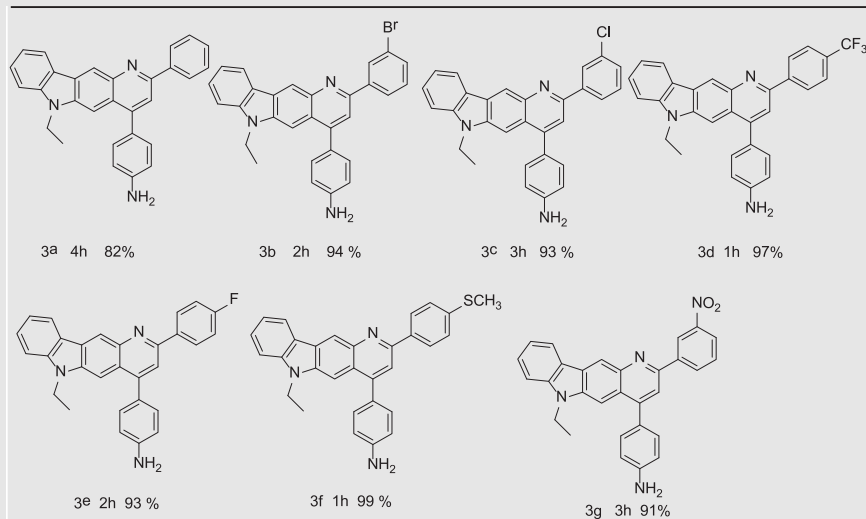
Teflon-lined stainless-steel autoclave, sealed, and heated at 116 °C for 3 h. During the process, the pressure was maintained at 30 psi and then dried in an oven at 130 °C for 3 h and calcined at 450 °C for 4 h in a muffle furnace, finally product was obtained.

3.4. General procedure for synthesis of (6*H*-pyrido[3,2-*b*]carbazol-4-yl)aniline derivatives

To a mixture of (*E*)-1-(4-aminophenyl)-3-phenylprop-2-en-1-one derivatives (1 mmol), 3-amino-9-ethylcarbazole (1 mmol), and sulfated Bi₂O₃-fly ash (100 mg) in water (20 mL) at 85 °C for 1–4 h, the completion of reaction was monitored by TLC. After completion the reaction mixture was cooled to room temperature, compound was separated with DCM. The organic layer was dried over on anhydrous Na₂SO₄, the excesses of solvent were removed. The crude products were purified by column chromatography, through silica gel (200 mesh) with (20%) 80:20 hexane/ethyl acetate as eluent afforded the desired pure products shown in Scheme 1. The purified products of **3a–3g** were confirmed by FT-IR, NMR (¹H, ¹³C), and LC–MS techniques. The heterogeneous nature of sulfated Bi₂O₃-fly ash catalyst was purified with DCM (30 mL) and dried in hot air oven at 130 °C for 1 h. After purification sulfated Bi₂O₃-fly ash catalyst was reused for further reaction.

3.5. Characterization data of (6*H*-pyrido[3,2-*b*]carbazol-4-yl)aniline derivatives (Table 2 entry **3a–3g**)

4-(6-Ethyl-2-phenyl-6*H*-pyrido[3,2-*b*]carbazol-4-yl)aniline (Table 2 entry 3a) Yield (339 mg 82%), brown solid, M.p. 258–259 °C; FT-IR (KBr, cm⁻¹) 3063, 2936, 1632, 1616; ¹H NMR (400 MHz, CDCl₃, δ ppm), 8.70 (s, 2H, NH₂), 8.18 (d, *J* = 7.68 Hz, 2H, ArH), 8.11 (d, *J* = 1.76 Hz, 2H, ArH),

Table 2 Synthesis of (6*H*-pyrido[3,2-*b*]carbazol-4-yl)aniline derivatives.^{a,b}

^a Reaction condition: (*E*)-1-(4-aminophenyl)-3-phenylprop-2-en-1-one derivatives (1 mmol), 3-amino-9-ethylcarbazole (1 mmol) and 100 mg of sulfated Bi₂O₃-fly ash in water (20 mL) were refluxed at 85 °C for 1–4 h.

^b Isolated yield (%).

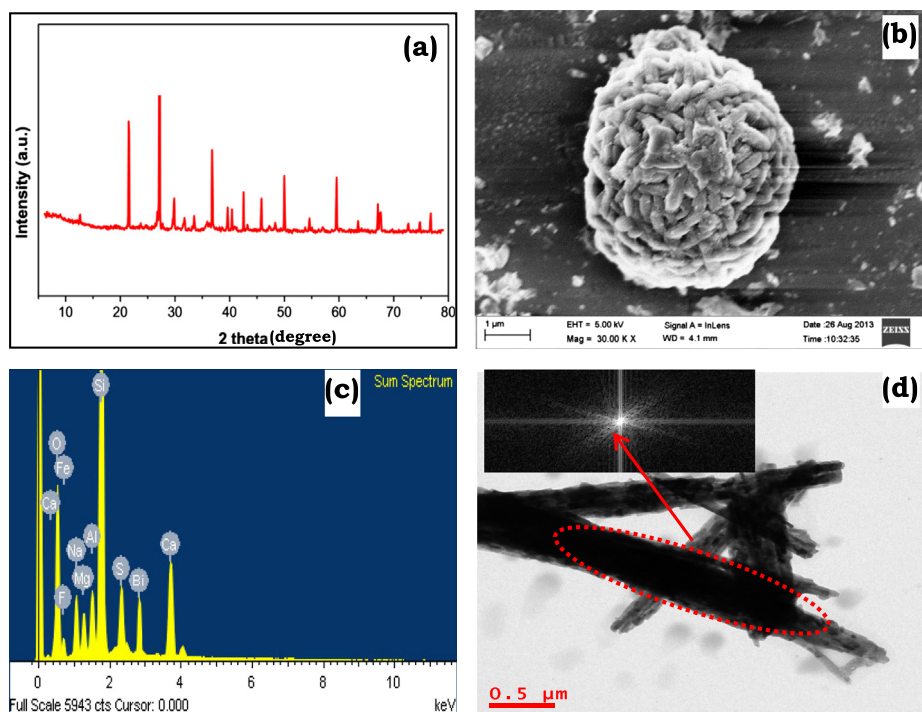


Figure 8 Reusability characterization of fifth run sulfated Bi_2O_3 -fly ash catalyst (a) powder XRD, (b) FE-SEM, (c) EDS and (d) TEM.

Table 3 Green metrics calculation for sulfated Bi_2O_3 -fly ash catalyzed synthesis of (6*H*-pyrido[3,2-*b*]carbazol-4-yl)aniline derivatives.

Entry	E-factor	Mass intensity	Atom economy	Atom efficiency
3a	0.04	1.54	97.40	79.86
3b	0.13	1.30	97.80	91.93
3c	0.14	1.33	97.81	90.96
3d	0.16	1.25	95.81	92.94
3e	0.15	1.34	97.73	90.88
3f	0.17	1.26	95.82	94.86
3g	0.08	1.39	94.43	85.93

$$\text{E - factor} = \frac{\text{Reactants total weight} - (\text{Product} + \text{Catalyst weight})}{\text{Product weight}}$$

8.04–8.01 (m, 3H, ArH), 7.90 (d, $J = 7.24$ Hz, 1H, ArH), 7.55–7.51 (m, 3H, ArH), 7.44–7.41 (m, 3H, ArH), 7.31 (t, $J = 7.48$ Hz, 2H, ArH), 4.38 (Q, $J = 7.21$ Hz, 2H, CH_2), 1.45 (t, $J = 7.20$ Hz, 3H, CH_3); ^{13}C NMR (100 MHz, CDCl_3 , δ ppm), 158.09, 143.82, 140.57, 138.87, 136.78, 130.94, 129.80, 128.83, 128.64, 125.96, 123.53, 123.13, 120.66, 120.06, 118.96, 112.65, 108.84, 108.75, 37.73, 13.94; LCMS m/z calculated for $\text{C}_{29}\text{H}_{23}\text{N}_3$ 413 found 413 [M].

4-(2-(3-Bromophenyl)-6-ethyl-6*H*-pyrido[3,2-*b*]carbazol-4-yl)aniline. (Table 2 entry 3b) Yield (463 mg 94%), brown solid, M.p. 292–293 °C; FT-IR (KBr, cm^{-1}) 3052, 2926, 1610; ^1H NMR (400 MHz, CDCl_3 , δ ppm), 8.60 (s, 2H, NH_2), 8.17 (s, 1H, ArH), 8.13 (d, $J = 7.81$ Hz, 1H, ArH), 8.06 (s, 1H, ArH), 7.84 (d, $J = 7.68$ Hz, 2H, ArH), 7.60 (d, $J = 7.92$ Hz, 2H, ArH), 7.51 (t, $J = 6.36$ Hz, 3H, ArH), 7.42 (d, $J = 8.52$ Hz, 3H, ArH), 7.37 (t, $J = 7.84$ Hz, 1H, ArH), 7.27 (t, $J = 6.82$ Hz, 1H, ArH), 4.35 (Q, $J = 7.21$ Hz, 2H, CH_2),

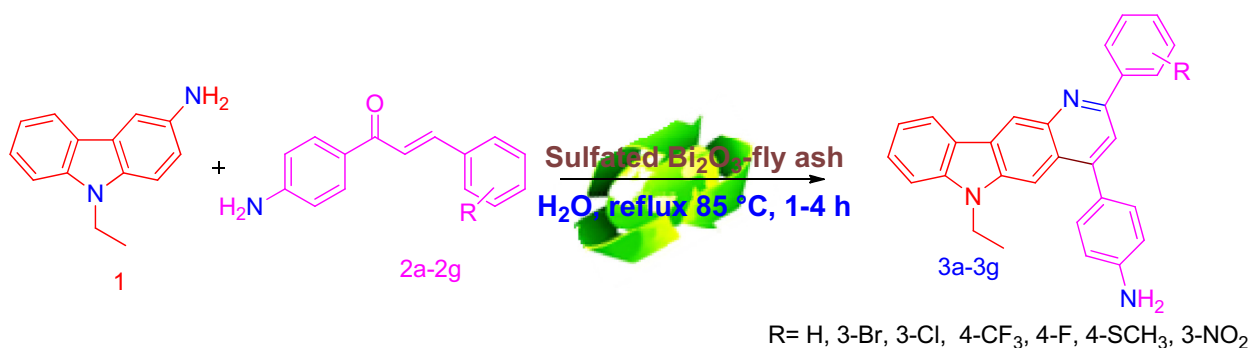
Table 4 Recycling potential of sulfated Bi_2O_3 fly ash for compound (3f).

Entry	No. of runs	Time (h)	Yield (%)	TON _S	TOF _S
1	Fresh	1	99	19.8	19.8
2	Run 1	1	99	19.8	19.8
3	Run 2	1	98	19.6	19.6
4	Run 3	1	98	19.6	19.6
5	Run 4	2	98	19.6	9.3
6	Run 5	2.5	97	18.4	7.36

1.45 (t, $J = 7.16$ Hz, 3H, CH_3); ^{13}C NMR (100 MHz, CDCl_3 , δ ppm), 155.85, 143.07, 140.55, 139.08, 138.76, 133.61, 131.03, 130.27, 127.36, 126.02, 123.51, 123.08, 120.62, 119.99, 119.03, 112.80, 108.85, 108.75, 37.75, 13.91; LCMS m/z calculated for $\text{C}_{29}\text{H}_{22}\text{BrN}_3$ 491 found 490 [M $^{-1}$].

4-(2-(3-Chlorophenyl)-6-ethyl-6*H*-pyrido[3,2-*b*]carbazol-4-yl)aniline (Table 2 entry 3c) Yield (418 mg 93%), brown solid, M.p. 273–274 °C; FT-IR (KBr, cm^{-1}) 3063, 2926, 1610; ^1H NMR (400 MHz, CDCl_3 , δ ppm), 8.62 (s, 2H, NH_2), 8.13 (d, $J = 7.72$ Hz, 2H, ArH), 8.05 (d, $J = 1.62$ Hz, 1H, ArH), 7.82–7.76 (m, 1H, ArH), 8.01 (s, 2H, ArH), 7.52–7.48 (m, 4H, ArH), 7.43 (t, $J = 1.56$ Hz, 3H, ArH), 7.27 (t, $J = 4.88$ Hz, 2H, ArH), 4.36 (Q, $J = 7.24$ Hz, 2H, CH_2), 1.45 (t, $J = 1.56$ Hz, 3H, CH_3); ^{13}C NMR (100 MHz, CDCl_3 , δ ppm), 156.00, 143.11, 140.55, 139.07, 138.53, 134.96, 130.71, 129.99, 128.08, 126.89, 126.01, 123.51, 123.05, 120.61, 119.99, 119.02, 108.84, 108.74, 37.75, 13.90; LCMS m/z calculated for $\text{C}_{29}\text{H}_{22}\text{ClN}_3$ 448 found 448 [M].

4-(6-Ethyl-2-(4-(trifluoromethyl)phenyl)-6*H*-pyrido[3,2-*b*]carbazol-4-yl)aniline (Table 2 entry 3d) Yield (471 mg 97%),



Scheme 1 Synthesis of (pyrido [3,2-b] carbazol-4-yl) aniline derivatives.

brown solid, M.p 285–286 °C; FT-IR (KBr, cm⁻¹) 3046, 2926, 1600; ¹H NMR (400 MHz, CDCl₃, δ ppm), 8.08 (d, *J* = 7.36 Hz, 1H, ArH), 8.05 (t, *J* = 8.36 Hz, 1H, ArH), 7.97 (d, *J* = 7.92 Hz, 1H, ArH), 7.79 (t, *J* = 8.20 Hz, 1H, ArH), 7.64 (s, 2H, ArH), 7.57 (s, 1H, ArH), 7.49 (d, *J* = 7.32 Hz, 1H, ArH), 7.43 (s, 1H, ArH), 7.38 (d, *J* = 8.00 Hz, 2H, ArH), 7.23 (d, *J* = 9.12 Hz, 2H, ArH), 6.93 (d, *J* = 8.28 Hz, 1H, ArH), 6.61 (d, *J* = 7.80 Hz, 1H, ArH), 4.25 (Q, *J* = 6.28 Hz, 2H, CH₂), 3.56 (s, 2H, NH₂), 1.38 (t, *J* = 6.92 Hz, 3H, CH₃); ¹³C NMR (100 MHz, CDCl₃, δ ppm), 155.80, 151.97, 142.94, 141.02, 140.50, 139.13, 138.79, 134.60, 131.32, 128.76, 128.40, 125.77, 125.59, 124.36, 123.72, 122.56, 120.54, 118.15, 115.78, 113.96, 109.16, 108.54, 106.45, 37.51, 13.36; LCMS *m/z* calculated for C₃₀H₂₂F₃N₃ 481 found 482 [M⁺].

4-(6-Ethyl-2-(4-fluorophenyl)-6H-pyrido[3,2-b]carbazol-4-yl)aniline (Table 2 entry 3e) Yield (403 mg 93%), brown solid, M.p 280–281 °C; FT-IR (KBr, cm⁻¹) 3052, 2931, 1605; ¹H NMR (400 MHz, CDCl₃, δ ppm), 8.63 (s, 2H, NH₂), 8.12 (d, *J* = 7.68 Hz, 1H, ArH), 8.03 (s, 2H, ArH), 7.97 (t, *J* = 6.56 Hz, 2H, ArH), 7.48 (d, *J* = 8.16 Hz, 3H, ArH), 7.42 (d, *J* = 8.36 Hz, 2H, ArH), 7.24 (t, *J* = 5.84 Hz, 3H, ArH), 7.17 (t, *J* = 8.36 Hz, 2H, ArH), 4.37 (Q, *J* = 7.20 Hz, 2H, CH₂), 1.45 (t, *J* = 7.28 Hz, 3H, CH₃); ¹³C NMR (100 MHz, CDCl₃, δ ppm), 165.68, 156.49, 143.59, 140.55, 138.85, 133.10, 130.50, 130.41, 125.93, 125.59, 123.51, 123.06, 120.58, 120.42, 119.94, 118.92, 118.73, 116.00, 115.78, 114.67, 112.47, 108.79, 108.79, 108.70, 108.42, 37.73, 13.88; LCMS *m/z* calculated for C₂₉H₂₂FN₃ 431 found 432 [M⁺].

4-(6-Ethyl-2-(4-(methylthio)phenyl)-6H-pyrido[3,2-b]carbazol-4-yl)aniline (Table 2 entry 3f) Yield (454 mg 99%), brown solid, M.p. 287–288 °C; FT-IR (KBr, cm⁻¹) 3353, 2931, 1589; ¹H NMR (400 MHz, CDCl₃, δ ppm), 8.04 (d, *J* = 7.28 Hz, 1H, ArH), 7.98 (d, *J* = 7.72 Hz, 1H, ArH), 7.82 (s, 1H, ArH), 7.48–7.54 (m, 3H, ArH), 7.43 (s, 1H, ArH), 7.38 (d, *J* = 7.68 Hz, 2H, ArH), 7.24 (s, 4H, ArH), 6.93 (d, *J* = 7.08 Hz, 1H, ArH), 6.61 (d, *J* = 7.76 Hz, 1H, ArH), 4.25 (Q, *J* = 6.80 Hz, 2H, CH₂), 3.58 (s, 2H, NH₂), 2.48 (s, 3H, SCH₃), 1.38 (t, *J* = 6.36 Hz, 3H, CH₃); ¹³C NMR (100 MHz, CDCl₃, δ ppm), 151.61, 142.62, 141.74, 140.49, 139.17, 134.58, 131.89, 131.15, 130.86, 129.03, 128.79, 128.29, 127.02, 126.02, 125.86, 125.57, 123.72, 122.57, 121.11, 120.56, 118.14, 115.77, 113.97, 109.16, 108.53, 106.44, 37.54, 15.17, 13.92; LCMS *m/z* calculated for C₃₀H₂₅N₃S 459 found 458 [M⁺].

4-(6-Ethyl-2-(3-nitrophenyl)-6H-pyrido[3,2-b]carbazol-4-yl)aniline (Table 2 entry 3g) Yield (419 mg 91%), brown solid, M.p. 284–285 °C; FT-IR (KBr, cm⁻¹) 3052, 2932, 1616; ¹H NMR (400 MHz, CDCl₃, δ ppm), 8.80 (s, 2H, NH₂, ArH), 8.76 (s, 1H, ArH), 8.32–8.30 (dd, *J*₁ = 1.76 Hz, *J*₂ = 1.76 Hz, 1H, ArH), 8.13 (d, *J* = 7.76 Hz, 1H, ArH), 8.10 (d, *J* = 1.96 Hz, 2H, ArH), 7.68 (t, *J* = 7.96 Hz, 1H, ArH), 7.55 (d, *J* = 2.04 Hz, 1H, ArH), 7.53 (d, *J* = 2.04 Hz, 1H, ArH), 7.51 (d, *J* = 1.04 Hz, 1H, ArH), 7.49 (d, *J* = 1.08 Hz, 1H, ArH), 7.46–7.43 (m, 2H, ArH), 7.29–7.25 (dd, *J*₁ = 14.81 Hz, *J*₂ = 14.72 Hz, 3H, ArH), 4.37 (Q, *J* = 7.20 Hz, 2H, CH₂), 1.45 (t, *J* = 7.21 Hz, 3H, CH₃); ¹³C NMR (100 MHz, CDCl₃, δ ppm), 154.20, 148.74, 142.41, 140.59, 139.37, 138.49, 134.62, 133.78, 129.73, 128.62, 126.13, 124.99, 123.55, 123.23, 123.02, 120.62, 120.03, 119.15, 113.05, 108.92, 108.81, 37.78, 13.90; LCMS *m/z* calculated for C₂₉H₂₂N₄O₂ 458 found 457 [M⁺].

4. Conclusions

In conclusion we report the sulfated Bi₂O₃-fly ash catalyst which was prepared by hydrothermal method. Environmentally challenge solid waste residue of fly ash was successfully recycled to catalyst application for the synthesis of (6H-pyrido[3,2-b]carbazol-4-yl)aniline derivatives **3a–3g** in water. Water and heterogeneous sulfated Bi₂O₃-fly ash were selected as catalyst due to environmental benign, reusable, easily separable, notable industrial applications. The sulfated Bi₂O₃-fly ash is most favorable to form adducts, hydrogen abstraction and cyclization. In addition the major component of Class C fly ash (SiO₂) may enhance the catalytic activity of oxidation processes. The reusability of sulfated Bi₂O₃-fly ash catalyst was examined up to five consecutive run. The result seems without any appreciable change in catalytic activity. The surface morphology and crystalline nature of reused sulfated Bi₂O₃-fly ash catalyst were characterized by Powder XRD, FE-SEM, EDS and TEM. From these studies, we have observed no noticeable changes in catalyst nature. Significance of sulfated Bi₂O₃-fly ash catalyst has been proved by hot filtration test method.

Acknowledgments

The Authors are gratefully acknowledge Prof. M. Periasamy, School of Chemistry, University of Hyderabad for the benevolent laboratory facility and also grateful to UGC Networking

Resource Centre, School of Chemistry, University of Hyderabad. One of the authors K.T. is grateful to School of Physics, University of Hyderabad for providing FE-SEM characterization. The authors also grateful to the Centre for Nanotechnology, University of Hyderabad for providing TEM measurements.

Appendix A. Supplementary material

Supplementary data associated with this article can be found, in the online version, at <http://dx.doi.org/10.1016/j.arabjc.2015.04.015>.

References

- Ai, Z., Huang, Y., Lee, S., Zhang, L., 2011. Monoclinic α -Bi₂O₃ Photocatalyst for efficient removal of gaseous NO and HCHO under visible light irradiation. *J. Alloys Comp.* 509, 2044–2049.
- Anastas, P.T., Beach, E.S., 2007. Green chemistry: the emergence of a transformative framework. *Green Chem. Lett. Rev.* 1, 9–24.
- Anastas, P., Eghbali, N., 2010. Green chemistry: principles and practice. *Chem. Soc. Rev.* 39, 301–312.
- Bothwell, J.M., Krabbe, S.W., Mohan, R.S., 2011. Applications of bismuth (III) compounds in organic synthesis. *Chem. Soc. Rev.* 40, 4649–4707.
- Dalton, L.K., Demerac, S., Elmes, B.C., Loder, J.W., Swan, J.M., Teitei, T., 1967. Synthesis of the tumor-inhibitory alkaloids, ellipticine, 9-methoxy ellipticine and related pyrido (4–3, b) carbazoles. *Aust. J. Chem.* 20, 2715–2722.
- Dijken, A.V., Bastiaansen, J.J.A.M., Kiggen, N.M.M., Langeveld, B.M.W., Rothe, C., Monkman, A., Bach, I., Stossel, P., Brunner, K., 2004. Carbazole compounds as host materials for triplet emitters in organic light-emitting diodes: polymer hosts for high-efficiency light-emitting diodes. *J. Am. Chem. Soc.* 126, 7718–7727.
- Ding, L., Balzarini, J., Schols, D., Meunier, B., Clercq, E.D., 1992. Anti-human immunodeficiency virus effects of cationic metalloporphyrin-ellipticine complexes. *Biochem. Pharm.* 44, 1675–1679.
- Dong, J.-L., Li, X.-H., Zhao, L.-J., Xiao, H.-S., Wang, F., Guo, X., Zhang, Y.-H., 2007. Raman observation of the interactions between NH₄⁺, SO₄²⁻, and H₂O in supersaturated (NH₄)₂SO₄ droplets. *J. Phys. Chem. B* 111, 12170–12176.
- Elkholy, M.M., Badawy, Z.I.El., Adawy, A.A.El., Deen, L.M.S.El., 1995. Optical absorption spectra studies for amorphous Cu₂O–Bi₂O₃ glass system. *J. Mater. Sci. Mater. Electron.* 6, 409–414.
- Gladysz, J.A., 2002. Introduction: recoverable catalysts and reagents—perspective and prospective. *Chem. Rev.* 102, 3215–3216.
- Gmouh, S., Yang, H., Vaultier, M., 2003. Activation of bismuth (III) derivatives in ionic liquids: novel and recyclable catalytic systems for Friedel–Crafts acylation of aromatic compounds. *Org. Lett.* 5, 2219–2222.
- He, F., He, Z., Xie, J., Li, Y., 2014. IR and Raman spectra properties of Bi₂O₃–ZnO–B₂O₃–BaO quaternary glass system. *Am. J. Anal. Chem.* 5, 1142–1150.
- Jain, D., Rani, A., 2011. MgO enriched coal fly ash as highly active heterogeneous base catalyst for Claisen–Schmidt Condensation reaction. *Am. Chem. Sci. J.* 2, 37–49.
- Jain, M., Mishra, M., Rani, A., 2012a. Synthesis and characterization of novel aminopropylated fly ash catalyst and its beneficial application in base catalyzed Knoevenagel condensation reaction. *Fuel Proc. Technol.* 95, 119–126.
- Jain, D., Mishra, M., Rani, A., 2012b. Synthesis and characterization of novel aminopropylated fly ash catalyst and its beneficial application in base catalyzed Knoevenagel condensation reaction. *Fuel Proc. Technol.* 95, 119–126.
- Kizek, R., Adam, V., Hrabeta, J., Eckschlager, T., Smutny, S., Burda, J.V., Frei, E., Stiborova, M., 2012. Anthracyclines and ellipticines as DNA-damaging anticancer drugs: Recent advances. *Pharm. Ther.* 133, 26–39.
- Liu, L., Jiang, J., Jin, S., Xia, Z., Tang, M., 2011. Hydrothermal synthesis of β -bismuth oxide nanowires from particles. *Cryst. Eng. Commun.* 13, 2529–2532.
- Lodeiro, I.G., Palomo, A., Jimenez, A.F., 2007. Alkali aggregate reaction in activated fly ash systems. *Cement. Conc. Res.* 37, 175–183.
- Lubineau, A., Auge, J., Queneau, Y., 1994. Water promoted organic reactions. *Synthesis*, 741–760.
- Anastas, P.T., Lankey R.L., 2002. (Eds.), In *Advancing Sustainability through Green Chemistry and Engineering*. ACS Symposium Series; American Chemical Society.
- Pin, F., Comesse, S., Garrigues, B., Marchalin, S., Daich, A., 2007. Intermolecular and intramolecular amidoalkylation reactions using bismuth triflate as the catalyst. *J. Org. Chem.* 72, 1181–1191.
- Qian, G., Song, Y., Zhang, C., Xia, Y., Zhang, H., Chui, P., 2006. Diopside-based glass–ceramics from MSW fly ash and bottom ash. *Waste Manage.* 26, 1462–1467.
- Roux, C.L., Iloughmane, H.G., Dubac, J., Jaud, J., Vignaux, P.J., 1993. New effective catalysts for Mukaiyama–Aldol and Michael reactions: BiCl₃–metallic iodide systems. *J. Org. Chem.* 58, 1835–1839.
- Roux, C.L., Iloughmane, H.G., Dubac, J., 1994. Bismuth (III) halide-catalyzed tandem Aldol halogenation reaction: a convenient synthesis of β -halo ketones and esters. *J. Org. Chem.* 59, 2238–2240.
- Sax, N.I., Bewis, R.J., 1989. *Dangerous Properties of Industrial Materials*. Van Nostrand Reinhold, New York, pp. 283–284.
- Sax, N.I., Bewis, R.J., 1989. *Dangerous properties of industrial materials*. Van Nostrand Reinhold, New York, pp. 522–523.
- Sillen, L.G., 1938. *Ark. Kemi, Mineral. Geol.* 12, 1.
- Sing, K.S.W., Everett, D.H., Haul, R.A.W., Moscou, L., Pierotti, R.A., Rouquerol, J., Siemieniowska, T., 1985. *Pure Appl. Chem.* 57, 603–619.
- Tanaka, H., Eguchi, H., Fujimoto, S., Hino, R., 2006. Two-step process for synthesis of a single phase Na-A zeolite from coal fly ash by dialysis. *Fuel* 85, 1329–1334.
- Thirunarayanan, G., Mayavel, P., Thirumurthy, K., 2012. Fly-ash: H₂SO₄ catalyzed solvent free efficient synthesis of some aryl chalcones under microwave irradiation. *Spectrochim. Acta A* 91, 18–22.
- Vistica, D.T., Kenney, S., Hursey, M.L., Boyd, M.R., 1994. Cellular uptake as a determinant of cytotoxicity of quarternalized ellipticines to human brain tumor Cells. *Biochem. Biophys. Res. Commun.* 200, 1762–1768.
- Wang, S., Wu, H., 2006. Environmental-benign utilisation of fly ash as low-cost adsorbents. *J. Hazard. Mater.* 136, 482–501.
- Wang, S., Li, L., Zhu, Z.H., 2007. Solid-state conversion of fly ash to effective adsorbents for Cu removal from wastewater. *J. Hazard. Mater.* 139, 254–259.
- Wang, J., Yang, X., Zhao, K., Xu, P., Zong, L., Yu, R., Wang, D., Deng, J., Chen, J., Xing, X., 2013. Precursor-induced fabrication of β -Bi₂O₃ microspheres and their performance as visible-light-driven photo catalysts. *J. Mater. Chem. A* 1, 9069–9074.
- Xie, T., Liu, C., Xu, L., Yang, J., Zhou, W., 2013. Novel heterojunction Bi₂O₃/SrFe₁₂O₁₉ magnetic photo catalyst with highly enhanced photocatalytic activity. *J. Phys. Chem. C* 117, 24601–24610.